J. Fluid Mech. (2008), *vol.* 596, *pp.* 191–200. © 2008 Cambridge University Press
doi:10.1017/S0022112007009548 Printed in the United Kingdom

Dynamics of an acoustically levitated particle using the lattice Boltzmann method

G. BARRIOS AND R. RECHTMAN

Centro de Investigación en Energía, Universidad Nacional Autónomade México, Apdo. Postal 34, Temixco, Morelos, 62580 Mexico
rrs@cie.unam.mx

(Received 7 June 2007 and in revised form 6 November 2007)

When the acoustic force inside a cavity balances the gravitational force on a particle the result is known as acoustic levitation. Using the lattice Boltzmann equation method we find the acoustic force acting on a rounded particle for two different single-axis acoustic levitators in two dimensions, the first with plane waves, the second with a rounded reflector that enhances the acoustic force. With no gravitational force, a particle oscillates around a pressure node; in the presence of gravity the oscillation is shifted a small vertical distance below the pressure node. This distance increases linearly as the density ratio between the solid particle and fluid grows. For both cavities, the particle oscillates with the frequency of the sound source and its harmonics and in some cases there is a much smaller second dominant frequency. When the momentum of the acoustic source changes, the oscillation around the average vertical position can have both frequencies mentioned above. However, if this quantity is large enough, the oscillations of the particle are aperiodic in the cavity with a rounded reflector.

1. Introduction

Acoustic levitation occurs when the acoustic force inside a cavity balances the gravitational force on a particle inside it. Acoustic levitation has been used to simulate microgravity conditions, for sample positioning, for non-contact measurements of liquid properties, and for fluid dynamics investigation of free drops (Chung & Trinh 1998; Hertz 1995; Trinh 1985; Brandt 2001).

The acoustic study of a particle in a sound wave was pioneered by King (1934), who found the force on a solid sphere due to travelling or standing acoustic plane waves and suggested the possibility of acoustic levitation in air. Gor'kov (1962) calculated the acoustic potential for a sphere in an ideal fluid and a standing wave from which the force over the sphere can be derived. Awatani (1955) was the first to report the radiation force over a cylinder due to a travelling wave for an ideal fluid and Wu *et al.* (1990) developed an expression for the case of a plane standing wave.

In this paper we show that the lattice Boltzmann method (LBM) (McNamara & Zanetti 1988; Higuera, Succi & Benzi 1989; Chen & Doolen 1998; Benzi, Succi & Vergassola 1992) can be used to study acoustic levitation. Since the stability of the trajectory of the levitated particle is of great interest in applications (Barmatz 1982; Rudnick & Barmatz 1990), we study the motion of a particle in two different two-dimensional cavities, one with a plane reflector, the other with a rounded one. We find that the stability of the trajectory depends on the geometry of the cavity, the density of the particle and the momentum added by the acoustic source.

https://doi.org/10.1017/S0022112007009548 Published online by Cambridge University Press

The LBM can simulate a compressible fluid with moving boundary conditions. On one hand, it is a compressible method (Alexander, Chen & Doolen 1992) capable of simulating acoustic waves with no modifications (Buick, Greated & Campbell 1998; Buick *et al.* 2000). On the other, Ladd (1994*a*, *b*) set up the basis for the study of the interaction between free macroscopic particles and the surrounding fluid by implementing no-slip boundary conditions between them. The total force exerted by the fluid on the particle can be calculated and the particle position and angular position updated. Aidun, Lu & Ding (1998) modified this model to improve the treatment of inertial effects and Filippova & Hanel (1997) developed an approximation to consider circular boundaries. Lattice Boltzmann simulations of the motion of a small cylinder in an ultrasound travelling field were carried out by Cosgrove *et al.* (2004). Haydock (2005*a*) developed a theory for the acoustic force on cylinders in an inviscid fluid and found a reasonable agreement with his LBM simulations when the viscous effects are negligible (Haydock 2005*b*). Both used the approach proposed by Ladd (1994*a*, *b*) for the no-slip boundary condition between particle and fluid, which limits the inertial effects of the solid particle. In the numerical simulations by Haydock (2005*b*) a solid particle was released inside a plane standing wave in the absence of a body force. The particle travelled to a pressure node, where the time-average acoustic force is zero.

In § 2 we briefly discuss the lattice Boltzmann method, mentioning the flows with which our numerical scheme was validated. In § 3 we present non-dimensional quantities and two different two-dimensional cavities for which numerical simulations were performed: one with a flat reflector the other with a rounded reflector similar to the one used by Xie & Wei (2001). Since our numerical simulations are two dimensional, the particle is an infinite cylinder. In § 4 we present numerical simulations of acoustic levitation in both cavities in the second resonant mode. In the absence of an external gravitational field, the particle oscillates around the pressure node in agreement with previous numerical simulations (Haydock 2005*b*). In the presence of an external gravitational field, the particle oscillates a small distance below the pressure node. We studied the behaviour of the particle when its density varies and the momentum density added by the acoustic source is constant, and when the density of the particle is fixed and the amplitude of the momentum density of the acoustic force varies (keeping all other parameters fixed). For the flat cavity we find that the particle always oscillates with the frequency of the acoustic source and its harmonics. For the rounded cavity and for large values of the amplitude of the momentum density added by the acoustic source, we find complex non-periodic trajectories.

2. The lattice Boltzmann equation method

In the $D2Q9$ model (see Qian, D'Humières & Lallemand 1992), space is discretized in a two-dimensional square lattice and only nine velocities are allowed: $\boldsymbol{c}_0 = (0, 0)$, $\boldsymbol{c}_1 = (1, 0)$, $\boldsymbol{c}_2 = (0, 1)$, $\boldsymbol{c}_3 = (-1, 0)$, $\boldsymbol{c}_4 = (0, -1)$, $\boldsymbol{c}_5 = (1, 1)$, $\boldsymbol{c}_6 = (-1, 1)$, $\boldsymbol{c}_7 = (-1, -1)$, and $\boldsymbol{c}_8 = (1, -1)$. The particle distribution functions $f_i(\boldsymbol{r}, t)$, at site $\boldsymbol{r}$, time t and velocity $\boldsymbol{c}_i$, $i = 0, \ldots, 8$, evolve according to the lattice Boltzmann equation

$$f_i(\boldsymbol{r} + \boldsymbol{c}_i, t + 1) - f_i(\boldsymbol{r}, t) = -\frac{1}{\tau}\left[f_i(\boldsymbol{r}, t) - f_i^{(eq)}(\boldsymbol{r}, t)\right] \tag{2.1}$$

where τ is the dimensionles relaxation time and $f_i^{(eq)}$ are the local equilibrium distribution functions,

$$f_i^{eq}(\boldsymbol{r}, t) = w_i \rho \left[1 + 3\boldsymbol{c}_i \cdot \boldsymbol{u} + \tfrac{9}{2}(\boldsymbol{c}_i \cdot \boldsymbol{u})^2 - \tfrac{3}{2}u^2\right]. \tag{2.2}$$

https://doi.org/10.1017/S0022112007009548 Published online by Cambridge University Press

In this equation $w_i = 4/9, 1/9, 1/36$ for $|\boldsymbol{c}_i| = 0, 1$ and $\sqrt{2}$ respectively, and ρ and $\boldsymbol{u}$ are the density and velocity defined by

$$\rho(\boldsymbol{r}, t) = \sum_{i=0}^{8} f_i(\boldsymbol{r}, t), \qquad \boldsymbol{u}(\boldsymbol{r}, t) = \frac{1}{\rho} \sum_{i=0}^{8} f_i(\boldsymbol{r}, t)\boldsymbol{c}_i. \tag{2.3}$$

The viscosity ν is related to the relaxation time τ by $\nu = c_s^2(\tau - 1/2)$, where $c_s = 1/\sqrt{3}$ is the speed of sound, and $p = \rho c_s^2$ where p is the pressure.

The right-hand side of (2.1) is a relaxation term that approximates Boltzmann's collision term (Bhatnagar, Gross & Krook 1954) and the first term on the left-hand side takes into account streaming to neighbouring sites. It is convenient to consider that during an iteration step, the fluid evolves by collisions (relaxations to local equilibrium) followed by streaming. To simulate the acoustic source of the levitator, the term $3w_i P c_{iy}$ is added to (2.1) at the sites of the lattice that coincide with the acoustic source. It is not hard to show that in the collision step this term introduces a change in momentum density $\Delta(\rho \boldsymbol{u})$ in the y-direction of magnitude P. In what follows we let P oscillate, $P = P_o \cos \omega_o t$, where P_o and ω_o are the amplitude and frequency of the momentum density applied at every site of the acoustic source. Taking this change of momentum per unit time and unit length we obtain the pressure density.

No-slip boundary conditions are simulated on the surface of the solid particle and the total force and torque are evaluated (Aidun *et al.* 1998) to find how the position of the particle and the angular velocity change. The walls of the cavity are simulated using bounce-back boundary conditions reversing the direction of the incoming distributions. To validate our numerical scheme we simulated several flows. We found good agreement with the results of the sedimentation of a circular particle in a narrow channel for different Reynolds numbers reported by Feng, Hu & Joseph (1994). We measured the acoustic force on a rigid cylinder in a plane standing wave and found good agreement with the results reported by Haydock (2005*b*), who had compared his numerical simulations with theoretical results (Haydock 2005*a*) and reported errors between 3 % and 146 % depending on the particle radius and the acoustic boundary layer thickness. Since the theory is valid for an inviscid fluid, the large errors reflect the fact that the numerical simulations fall outside the domain of validity of the theory. Haydock used Ladd's approach to treat the boundary between the fluid and the particle based on bounce-back boundary conditions and we used Aidun's proposal based on half-way bounce-back boundary conditions which are known to give better results.

To determine an appropriate lattice size, we compared our results with those of Poe & Acrivos (1975) for the rotation of a particle in Couette flow. When the radius of the particle is 9.5 lattice units, we found an error smaller than 3 %. On the other hand, in acoustic levitation in a rounded three-dimensional cavity Xie & Wei (2001) used a particle of 2 mm radius.

3. Dimensionless quantities and acoustic levitators

The dimensionless quantities for the acoustic levitation problem, denoted by an asterisk, are

$$x^* = kx, \qquad y^* = ky, \qquad r^* = kr, \qquad t^* = t/T \tag{3.1}$$

https://doi.org/10.1017/S0022112007009548 Published online by Cambridge University Press

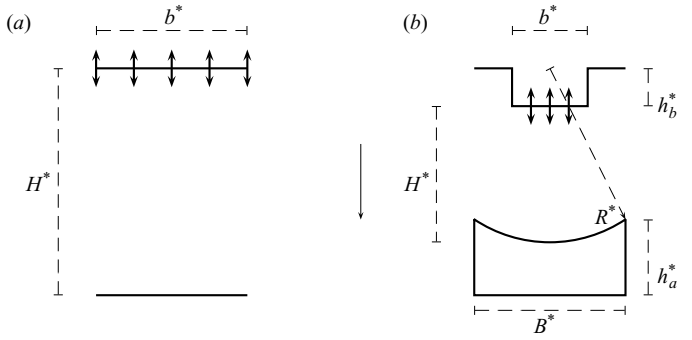


FIGURE 1. (*a*) Single-axis acoustic levitator with a plane reflector. The vibrating source is located at the top of the cavity; $b^* = 5.092$. (*b*) Single-axis acoustic levitator with a rounded reflector with $b^* = 5.092$, $B^* = 2b^*$, $R^* = 12.244$, $h_b^* = 0.1377$, $W^* = 30$, and $h_a^* = 0.01028$. For both cavities H^* is adjusted to the second resonant mode, $\tau = 0.6$, and $\rho_f = 0.6$.

where x, y, r and t are the horizontal and vertical position, the radius of the particle, and time respectively, T is the period and $k = 2\pi/\lambda$ is the wavenumber with λ the wavelength of the standing wave. The dimensionless momentum density P^* is

$$P^* = \frac{PkT}{\pi r^2 \rho_f}, \tag{3.2}$$

where ρ_f is the fluid density.

Numerical simulations were carried out in two different single-axis acoustic cavities shown schematically in figure 1(*a*, *b*). The first is formed by a plane vibrating source at the top and a plane reflector at the bottom with periodic boundary conditions in the horizontal direction. The second cavity has the same shape and parameters as the one presented by Xie & Wei (2001) but in two dimensions. The vertical walls are far from the acoustic source. Since b^* has the same value in both cavities, the acoustic source inputs are equal.

4. Numerical simulations

The first step is to establish ω_o, the frequency of a standing wave in the second resonant mode in both cavities without a particle. We generate a standing wave by adding momentum at the sites of the vibrating source periodically, $P^* = P_o^* \cos \omega_o t$, as mentioned in § 2. The initial conditions for the numerical simulations are different for each cavity. For the flat cavity, we start with a given velocity and pressure profile, knowing that in a standing wave the phase differs by $\pi/2$ and that $v_1 = p_1/\rho_f c_s$ with v_1 and p_1 the velocity and pressure amplitudes ($p_1 \propto P_o$). Then $\omega_o = 6\pi c_s/4H$ where H is the height of the cavity (Strutt & Rayleigh 1945). For the rounded cavity, we start with the fluid at rest and add momentum periodically to the acoustic source of the levitator. After approximately 300 periods a standing wave is formed inside the cavity and we measure the maximum velocity amplitude. In the resonant modes the velocity amplitude is a maximum and this gives us the value of ω_o for the second resonant mode.

In the absence of an external gravitational field, a particle will move to a pressure node. In the presence of gravity, the particle's stationary vertical position is shifted to where the time-average acoustic force on the particle is equal to its weight. In figure 2(*a*, *b*) we show the vertical positions of several particles for both cavities.

https://doi.org/10.1017/S0022112007009548 Published online by Cambridge University Press

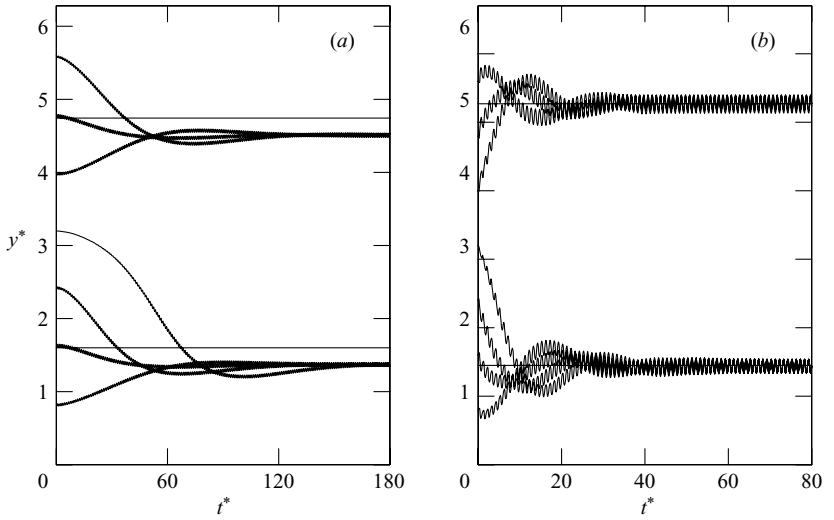


FIGURE 2. Vertical positions of particles with $r^* = 0.25$ and twice the density of the fluid in the presence of gravity for (*a*) the flat cavity and (*b*) the rounded one. The horizontal lines represent the vertical position of the pressure node. The oscillations in the flat cavity are barely visible. For both cavities $P_o^* = 1.6 \times 10^{-3}$. Lattices of 163×201 and 901×251 nodes were used for the flat and rounded cavity respectively.

The horizontal lines indicate the position of the pressure nodes. The displacement of the stationary position from the pressure node is larger in the flat cavity than in the rounded one, where it is barely noticeable. However, we find larger oscillations in the latter.

In the following, we report the results of numerical simulations in the second resonant mode with the particle initially near the pressure node closest to the reflector. In figure 3(*a*, *b*) we show y_s^*, the time average of the vertical position of the particle after a long transient, as the ratio of the density of the particle ρ_p and the fluid ρ_f varies for a fixed value of P_o^*. We also show the standard deviation, which is a measure of the amplitude of oscillation of the particle around y_s^*. There is a near-linear behaviour in both cavities, which implies that the mean acoustic force is proportional to the deviation of y_s^* from the pressure node. A detailed analysis of all trajectories indicates the presence of a small-amplitude oscillation with frequency ω_o and its harmonics. The large values of the standard deviation of y_s^* in the rounded cavity for $50 \lesssim \rho_p/\rho_f \lesssim 250$ are the consequence of large-amplitude oscillations of frequency ω_1 and its harmonics with $\omega_1 \ll \omega_o$.

In figure 4(*a*, *b*) we show y_s^* with its standard deviation as P_o^*, the amplitude of the applied external momentum varies, keeping ρ_p/ρ_f fixed. As P_o^* grows, y_s^* approaches the pressure node in the flat cavity. For the rounded cavity, the situation is more complex, since the pressure node's position depends on P_o^* as we also show in figure 4(*b*). To explain the results found for the rounded cavity we show the vertical positions for three values of P_o^* in figure 5. In figures 5(*a*) and 5(*b*) there is a small-amplitude oscillation with frequency ω_o and its harmonics, while in figure 5(*c*) this oscillation has been filtered out. In figure 5(*a*), that corresponds to the smallest value of P_o^* in figure 4(*b*), the power spectrum shows a second frequency ω_1, much smaller than ω_o, together with its harmonics. These low-frequency oscillations are present in all the numerical simulations reported in figure 4(*b*) except the one for the largest value of P_o^*. In figure 5(*b*), for P_o^* where the standard deviation of y_s^*

https://doi.org/10.1017/S0022112007009548 Published online by Cambridge University Press

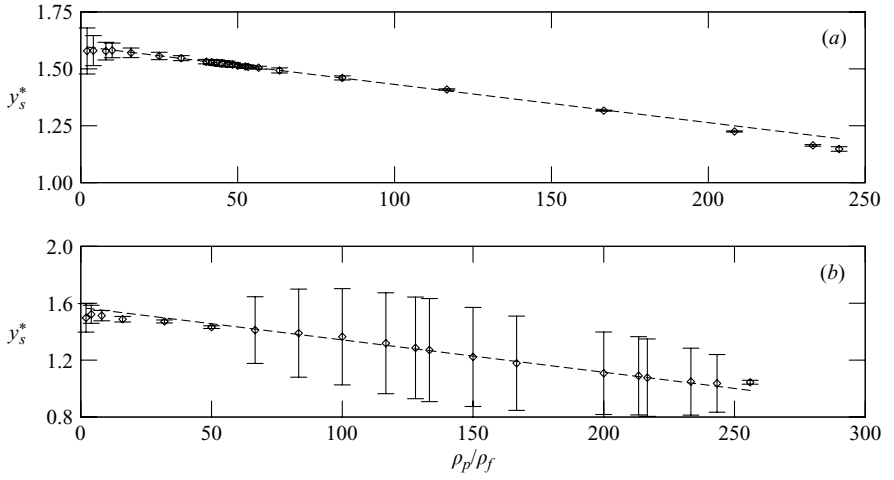


FIGURE 3. Vertical stationary position y_s^* with its standard deviation as ρ_p/ρ_f varies for (a) the flat and (b) the rounded cavity. In the numerical simulations $P^* = 0.01$ for the flat cavity and $P^* = 0.0019$ for the rounded one. The slopes of the linear fit are (a) -0.00168 and (b) -0.00227.

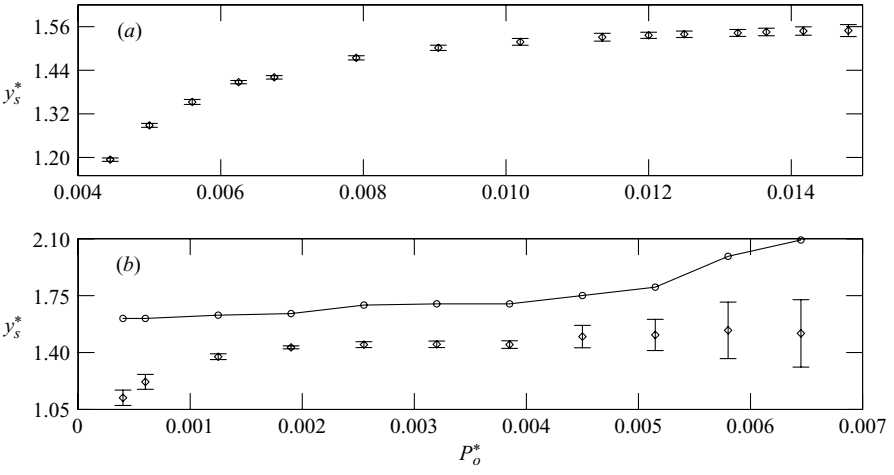


FIGURE 4. Vertical stationary position y_s^* with its standard deviation as P_o^* varies with $\rho_p/\rho_f = 50$ for the (a) flat and (b) rounded cavities. In the flat cavity, the pressure node is at $y^* = 1.6$. The curve in (b) shows the vertical position of the pressure node.

in figure 4(b) begins to grow, and 5(c), for the last value of P_o^* in that figure the oscillations are more complex. The origin of this change is the horizontal motion of the particle, which was not present before, due to a doubling of the pressure node nearest the rounded reflector for $P_o^* > P_{o_c}^*$ with $P_{o_c}^*$ between 0.0032 and 0.0038 as we show in figure 6. For $P_o^* > P_{o_c}^*$, except for the last value of P_o^* shown in figure 4(b), the particle oscillates horizontally with frequencies ω_o and its harmonics and a much smaller frequency ω_2 and its harmonics.

The particle oscillation for the largest value of P_o^* of figure 4(b) is qualitatively different from the others. In figure 5(c) and 5(d) we show the vertical and horizontal motion of the particle. Large-amplitude horizontal oscillations correspond to

https://doi.org/10.1017/S0022112007009548 Published online by Cambridge University Press

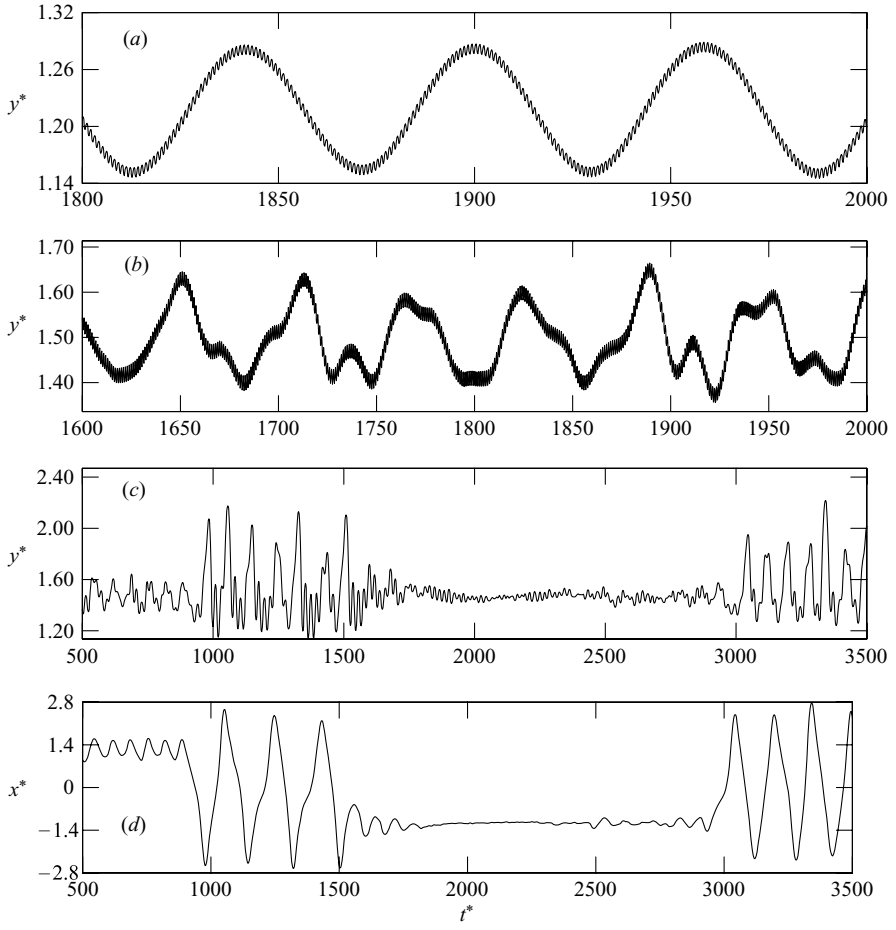


FIGURE 5. Vertical positions for (*a*) $P_o^* = 6.0 \times 10^{-4}$ and (*b*) $P_o^* = 4.5 \times 10^{-3}$. Vertical (*c*) and horizontal (*d*) positions of a particle with $P_o^* = 6.45 \times 10^{-3}$. In all three simulations, $\rho_p/\rho_f = 50$ for the rounded cavity.

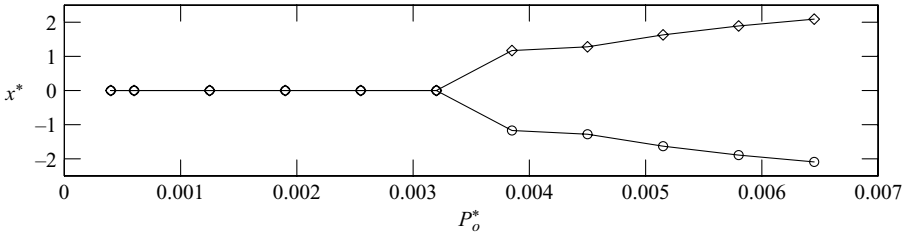


FIGURE 6. Horizontal position of the pressure node with $\rho_p/\rho_f = 50$. We find $P_{o_c}^*$ between 0.0032 and 0.0038.

large-amplitude vertical oscillations. The particle oscillates horizontally near one of the pressure nodes, then it oscillates around both of them until it is attracted by the other one. This behaviour continues irregularly for a long time, which is not shown in the figure, and eventually ($t^* > 16\,000$) the particle oscillates between the two pressure nodes. Evidence of the aperiodic vertical oscillations can be found in the

https://doi.org/10.1017/S0022112007009548 Published online by Cambridge University Press

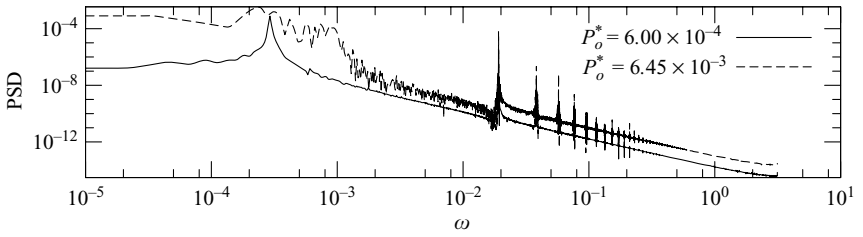


FIGURE 7. Power spectra of the vertical motion shown in figure 5(*a*) (continuous curve) with $\omega_o = 0.019126$ and $\omega_1 = 0.0002913$ and (dashed curve) in figure 5(*c*) with the same value of ω_o.

power spectrum shown in figure 7 where we cannot identify a frequency ω_1, in contrast to the power spectrum for the vertical motion of the particle shown in figure 5(*a*) for which ω_1 is clearly distinguishable. From the time series of the horizontal or vertical position of the particle we evaluated the largest Lyapunov exponent and found a value much too small to conclude that the motion of the particle is chaotic (Hegger, Kantz & Schreiber 1999; Kantz & Schreiber 2004). It is possible that there is a chaotic transient (Strogatz 1994) or a complex behaviour even if the maximum Lyapunov exponent is zero.

5. Concluding remarks

The lattice Boltzmann method can describe the interaction of a compressible fluid with a solid moving particle in acoustic levitation. We performed numerical simulations for varying ratio of densities of the particle and fluid and a fixed value of the momentum density added by the acoustic source for flat and rounded cavities. The average height at which the particle oscillates varies linearly with the density ratio for both cavities. The particle oscillates with the frequency of the acoustic source and its harmonics and in some cases with a much smaller frequency. When the momentum density of the acoustic source is varied for a fixed value of the density ratio, the particle in the flat cavity oscillates around a vertical position that approaches the pressure node as the momentum increases, again with the frequency of the acoustic source and its harmonics and in some cases with a smaller frequency. For the rounded cavity, the appearance of two pressure nodes destabilizes the oscillation which may become aperiodic due to the horizontal motion of the particle around the two pressure nodes. We speculate that the particle is the source of an asymmetric horizontal force that gives rise to such an aperiodic behaviour. We could not find a chaotic motion but we did not explore the whole parameter space.

Altough we have focused on the motion of the particle, we could also focus on the fluid. For example, we measured the streaming velocity, defined as the time-averaged velocity at a site, and our results agree with those of Haydock (2005*a*), who found that the maximum streaming velocity is almost 2 % of the maximum velocity inside the cavity.

The numerical simulations show that the rounded cavity is more efficient in the sense that levitation occurs with a smaller value of the momentum density added by the acoustic force than in the square cavity, as is expected. But the price for this efficiency is larger oscillations of the particle that lead to a complex non-periodic motion, caused by the doubling of the pressure node.

Using the LBM, simulations in complicated geometries can be carried out. These may help to determine the shift in the resonant frequency due to the presence of

https://doi.org/10.1017/S0022112007009548 Published online by Cambridge University Press

a particle and optimize the geometry of the reflector for a single- or multiple-axis levitator. Another advantage of the method is that it can be directly extended to three dimensions.

The authors thank Guadalupe Huelsz for suggesting the study of acoustic levitation and proofreading the manuscript. The authors also thank Héctor Cortés, Francisco Mandujano, Eduardo Ramos, and Jorge Rojas for fruitful discussions and suggestions. Partial economic support from CONACyT project U41347 is acknowledged. G. Barrios thanks CONACyT for a postgraduate scholarship.

REFERENCES

Aidun, C., Lu, Y. & Ding, E. 1998 Direct analysis of particulate suspensions with inertia using the discrete Boltzmann equation. *J. Fluid Mech.* **373**, 287–311.

Alexander, F., Chen, H. & Doolen, G. 1992 Lattice Boltzmann model for compressible fluids. *Phys. Rev.* A **46**, 1967–1970.

Awatani, J. 1955 Study on acoustic radiation pressure (iv) (radiation pressure on a cylinder). *Mem. Inst. Sci. Osaka University* **12**, 95–102.

Barmatz, M. 1982 Overview of containerless processing technologies. In *Materials Processing in the Reduced Gravity Environment of Space* (ed. G. E. Ridone). Elsevier.

Benzi, R., Succi, S. & Vergassola, M. 1992 The lattice Boltzmann equation: Theory and applications. *Physi. Rep.* **222**, 145–197.

Bhatnagar, P. L., Gross, E. P. & Krook, M. 1954 A model for collision processes in gases. I. Small amplitude processes in charged and neutral one-component systems. *Phys. Rev.* **94**, 511–525.

Brandt, E. 2001 Suspended by sound. *Nature* **413**, 474–475.

Buick, J., Buckley, C., Greated, C. & Gilbert, J. 2000 Lattice Boltzmann BGK simulations of nonlinear sound waves: the development of a shock front. *J. Phys.* A*: Math. Gen.* **33**, 3917–3928.

Buick, J., Greated, C. & Campbell, D. 1998 Lattice BGK simulation of sound waves. *Europhys. Lett.* **43**, 235–240.

Chen, S. & Doolen, G. D. 1998 Lattice Boltzmann method for fluid flows. *Annu. Rev. Fluid Mech.* **30**, 329–364.

Chung, S. & Trinh, E. 1998 Containerless protein crystal growth in rotating levitated drops. *J. Cryst. Growth* **194**, 384–397.

Cosgrove, J., Buick, J., Campbell, D. & Greated, C. 2004 Numerical simulation of particle motion in an ultrasound field using the lattice Boltzmann model. *Ultrasonics* **43**, 21–25.

Feng, J., Hu, H. H. & Joseph, D. D. 1994 Direct simulation of initial value problems for the motion of solid bodies in a Newtonian fluid Part 1. Sedimentation. *J. Fluid Mech.* **261**, 95–134.

Filippova, O. & Hanel, D. 1997 Lattice-Boltzmann simulation of gas-particle flow in filters. *Computers Fluids* **26**, 697–712.

Gor'kov, L. P. 1962 On the forces acting on a small particle in an acoustical field in an ideal fluid. *Sov. Phys.* **6** (9), 773–775.

Haydock, D. 2005*a* Calculation of the radiation force on a cylinder in a standing wave acoustic field. *J. Phys.* A*: Math. Gen.* **38**, 3279–3285.

Haydock, D. 2005*b* Lattice Boltzmann simulations of the time-averaged forces on a cylinder in a sound field. *J. Phys.* A*: Math. Gen.* **38**, 3265–3277.

Hegger, R., Kantz, H. & Schreiber, T. 1999 Practical implementation of nonlinear time series methods: The TISEAN package. *Chaos* **9**, 413–435.

Hertz, H. 1995 Standing-wave acoustic trap for nonintrusive positioning of microparticles. *J. App. Phys.* **78**, 4845–4849.

Higuera, F. J., Succi, S. & Benzi, R. 1989 Lattice gas dynamics with enhanced collisions. *Europhys. Lett.* **9**, 345–349.

Kantz, H. & Schreiber, T. 2004 *Nonlinear Time Series Analysis*. Cambridge.

King, L. V. 1934 On the acoustic radiation pressure on spheres. *Proc. R. Soc. Lond.* A **147**, 212–240.

https://doi.org/10.1017/S0022112007009548 Published online by Cambridge University Press

Ladd, A. J. C. 1994*a* Numerical simulations of particulate suspensions via a discretized Boltzmann equation. Part 1. Theoretical foundation. *J. Fluid Mech.* **271**, 285–309.

Ladd, A. J. C. 1994*b* Numerical simulations of particulate suspensions via a discretized Boltzmann equation. Part 2. Numerical results. *J. Fluid Mech.* **271**, 311–339.

McNamara, G. & Zanetti, G. 1988 Use of the Boltzmann equation to simulate lattice gas automata. *Phys. Rev. Lett.* **61**.

Poe, G. G. & Acrivos, A. 1975 Closed streamline flows past rotating single cylinder and spheres: intertia effect. *J. Fluid Mech.* **72**, 605.

Qian, Y. H., D'Humières, D. & Lallemand, P. 1992 Lattice BGK models for Navier-Stokes equations. *Europhys. Lett.* **17**, 479–484.

Rudnick, J. & Barmatz, M. 1990 Oscillational instabilities in single-mode acoustic levitators. *J. Acoust. Soc. Am.* **87**, 81–92.

Strogatz, S. H. 1994 *Nonlinear Dynamics and Chaos with Applications to Physics, Biology, Chemistry and Engineering*. Perseus Books.

Strutt, J. W. & Rayleigh, Lord 1945 *The Theory of Sound*. Dover.

Trinh, E. H. 1985 Compact acoustic levitation device for studies in fluid dynamics and material science in the laboratory and microgravity. *Rev. Sci. Instrum.* **56**, 2059–2065.

Wu, J., Du, G., Work, S. & Warshaw, D. 1990 Acoustic radiation pressure on a rigid cylinder: An analytical theory and experiments. *J. Acoust. Soc. Am.* **87**, 581–586.

Xie, W. & Wei, B. 2001 Parametric study of single-axis acoustic levitation. *App. Phys. Lett.* **79**, 881–883.

https://doi.org/10.1017/S0022112007009548 Published online by Cambridge University Press